Instanton-induced inelastic collisions in QCD

Maciek A. Nowak
M. Smoluchowski Institute of Physics, Jagellonian University, Cracow, Poland
and Department of Physics and Astronomy, State University of New York, Stony Brook, New York 11794

Edward V. Shuryak and Ismail Zahed
Department of Physics and Astronomy, State University of New York, Stony Brook, New York 11794
(Received 24 January 2001; published 3 July 2001)

We show that the instanton-induced inelastic processes, leading to multigluon production in high-energy parton-parton scattering, are considerably enhanced (by a factor of 100) over the quasielastic ones. The basic instanton-induced inelastic contribution causes the parton-parton cross section to increase as $\ln s$, due to prompt production of multigluon clusters of mass 2–3 GeV close to QCD sphalerons. The cross section is related to the Pomeron slope and intercept in the usual parametrization, which are evaluated. We show that the small intercept is due to the diluteness of the instantons in the QCD vacuum, while the small size of the Pomeron (seen via its slope) is related to the smallness of the instanton sizes.

DOI: 10.1103/PhysRevD.64.034008 PACS number(s): 13.85.−t, 11.15.Kc

I. INTRODUCTION

QCD instantons [1,2] play an important role in the composition of the vacuum and its hadronic excitations [3]. This viewpoint is strongly supported by detailed lattice simulations [3]. Naturally most hadronic substructures, whether in the form of constituent quarks or gluons, should also be important for hadronic reactions at high energies. A somewhat different program of looking for direct manifestation of small-size instantons in deep-inelastic collisions is pursued at the DESY ep collider HERA, see Ref. [13].

The problem in translating vacuum physics to high-energy scattering has been strongly limited by technical issues, an important one being the Euclidean nature of instanton physics and the inherent light-cone character of high-energy kinematics. As a result, the theory of high-energy processes remains mostly perturbative, as best illustrated by the Balitskiĭ-Fadin-Kuraev-Lipatov (BFKL) ladder resummation [4] in the hard regime, with exchange momenta much larger than 1 GeV.

A rich Pomeron phenomenology has been developed prior and through QCD. We will not be able to render justice here to all relevant papers. Particularly important for us is the formulation based on the eikonal expansion for the high-energy parton-parton cross section, originally suggested by Nachtmann [5]. Similar expressions for structure functions were also suggested by Muller [6]. Ideas using instanton effects for high-energy QCD processes were also recently discussed, for dipole cross sections in Ref. [7], and the soft Pomeron problem in Refs. [8] and [9] [Kharzeev-Kovchegov-Levin (KKL)].

Recently, we have suggested a nonperturbative approach to high-energy scattering using instantons [10]. The eikonalized near-forward parton-parton scattering amplitude was reduced to a pertinent correlation function of two (or more) straight Wilson lines, which were analyzed in Euclidean space using instantons. The lines lie at an arbitrary angle θ, which is then analytically continued to Minkowski space by the trick $y=-i\theta$ where y is the Minkowski rapidity. A similar construction was applied recently to nonperturbative parton-parton scattering in supersymmetric theories using the AdS conformal field theory (CFT) correspondence [11], where on the boundary large N instantons are expected to saturate exactly the diffractive cross section. (Incidentally, most of the arguments to follow can be checked exactly in these theories using the instanton calculus.) In the instanton field the parton Wilson lines involve multigluon exchange as depicted in Fig. 1, with no need for initial and final state multigluon resummation. Our analysis has shown that the cross section for ''quasielastic'' (color-transfer) parton-parton and dipole-dipole scattering is constant at large $\sqrt{s}$.

In this paper we extend our original analysis to ''truly inelastic'' parton-parton scattering amplitudes, with prompt

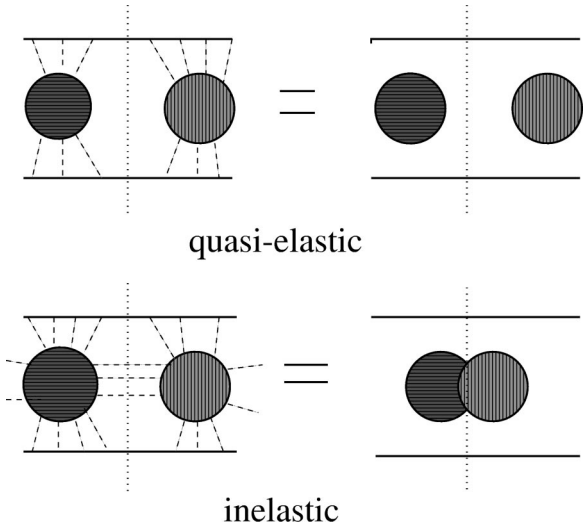

FIG. 1. Schematic representation of the amplitude squared, with (without) gluon lines are shown in the left (right) side of the figure. The dotted vertical line is the unitarity cut. The upper panel illustrates the quasielastic (at the parton level) amplitudes where only color is exchanged as detailed in Ref. [10]. The lower panel depicts inelastic processes in which some gluons cross the unitarity cut, and some gluons are absorbed in the initial stage.

parton production. Such partonic processes have new particle lines crossing the unitarity cut as shown in the lower-left part of Fig. 1. Similar processes have been considered in the context of baryon-number violation in the electroweak theory [12]. In the latter it was shown that multiple gluon production can also be calculated semiclassically, through interacting instanton–anti-instanton configurations or streamlines [14] which interpolate between a well separated instanton–anti-instanton and the vacuum. By combining the semiclassical treatment of multiple incoming gluons, as done in Ref. [10], with the streamline-based treatment of multiple outgoing gluons, we can completely bypass the perturbative expansion, as indicated in the lower-right part of Fig. 1. Contacts with perturbation theory follow by expanding the instanton contributions in powers of the field in the weak-field limit.

In this paper we will not develop a quantitative theory of hadronic collisions (as that requires further modeling) and consider only the basic process involving inelastic quark-quark scattering. For clarity, it is important that the underlying assumptions in our analysis be spelled out from the onset. Throughout, the scattering processes are understood to undergo three sequential stages.

(i) Initial stage: Partons are initially described by some wave function in a fixed frame (say the c.m.), depending on their transverse momenta and rapidities.[1] The *through-going partons* should be formed outside of the instanton of mean size ρ_0 with $k_\perp^2/\sqrt{s} \leqslant 1/\rho_0$, while the *wee partons* (the opposite condition) are not in the wave function but included in the cross section. The former are assumed to move along the eikonalized straight Wilson lines, while the latter are part of the process.

(ii) Prompt stage: In it the incoming partons pass each other. Color of throughgoing partons could be changed (quasielastic), or new partons/hadrons could appear (inelastic). In analogy with the perturbative treatment, confinement is ignored at this stage, since the passage time is short (of order $1/\sqrt{s}$). All partons interact with instantons.

(iii) Final stage: In it all produced partons fly away, some dragging longitudinal color strings of matching color. String breaking happens with probability one, thus cross sections are not affected. These eventually produce the hadronic final states and multiplicities. All partonic amplitudes to be assessed will take place in the prompt regime. We assume that by duality, the total partonic cross sections match the hadronic cross sections.

In Sec. II, we give an overview of the salient physical points of this work. In Sec. III, we give a brief account of the instanton-induced quasielastic (color-transfer), parton-parton scattering amplitude as reported in Ref. [10]. We also report on novel issues regarding the character of the weak-field limit in light of perturbation theory, as well as the absence of odderons in instanton-induced processes. In Sec. IV we argue that the full inelastic contribution to the parton-parton scattering amplitude follows semiclassically from the QCD streamline configuration. The result is a remarkable enhancement in the inelastic scattering amplitude, limited only by the unitarity bound. In Sec. V we show that a statistical resummation of the enhanced pair cross sections yield a Reggeized hadron-hadron scattering cross section. The Pomeron intercept and slope are sensitive to the QCD vacuum parameters, and as it turns out, even to the instanton shapes. In Sec. VI we draw a parallel between the Weizsacker-Williams approximation to inelastic scattering and the weak-field limit of the semiclassical analysis, and argue that the instanton-induced form factors used recently in Ref. [9] are not the pertinent ones. In Sec. VII we discuss additional contributions to the diffractive process not retained in our analysis. Our conclusions and outlook are summarized in Sec. VIII.

II. PHYSICAL HIGHLIGHTS

The ubiquitous character of the instantons in the nonperturbative QCD vacuum, as now established both theoretically and numerically, leads naturally to their importance in partonic scattering during the collision time (prompt stage). In particular, instantons prove essential for discriminating perturbative from nonperturbative effects. Indeed, whenever instanton effects are included (even in lowest order) one can often locate the nonperturbative boundary in perturbation theory, and even makes meaningful predictions a little beyond it [3]. Although in QCD instanton-induced effects have a small amplitude (density) $n_0 \approx e^{-2\pi/\alpha_s}$, they correspond to strong (classical) fields $A \approx 1/g$. Hence any interaction with a parton of charge g is $gA \approx 1$ which is independent of the charge. In contrast to perturbation theory, there is no additional penalty for adding partons to the amplitude. Therefore the instanton-induced amplitudes overcome the perturbative amplitudes at high enough order. Indeed, recently we have suggested [10] that instantons would dominate collisions with multiple color exchanges between partons, leading to the higher observed hadronic multiplicities.

The important question regarding the transition from the perturbative regime to the instanton dominated (semiclassical) regime in parton-parton collisions depends critically on the numerical parameters characterizing the QCD vacuum. There are essentially two key parameters [15] (see also Ref. [10] for some details). The instanton (plus anti-instanton) density $n_0 \approx 1/\mathrm{fm}^4$ and the mean instanton size $\rho_0 \approx 1/3$ fm yield the dimensionless diluteness $\kappa_0 = n_0 \rho_0^4 \approx 0.01$ of the instanton vacuum.[2] The mean instanton action is $S_0 = 2\pi/\alpha_s \approx 10$–$15$. Each time an instanton is inserted it costs a small factor κ_0. However, there are no coupling constants, and so each time we compare the results with their perturbative counterparts we get powers of the large action S_0, with a net

[1]The parton model is of course frame and scale specific: partons which belong to a wave function of one colliding hadron in a given frame can belong to another hadron wave function in another frame. The normalization scale is basically given by the inverse instanton size.

[2]For comparison we note that in the electroweak theory the diluteness factor is 10^{-84} despite the fact that the coupling is only three times smaller than in QCD.

gain per gluon involved. Numerically the instanton-induced effects should dominate the perturbative effects from third order and on ($\kappa_0 S_0^2 \approx 1$), while they are comparable to second order. Of course this argument is too naive; there may be other factors and so on, but we believe the argument captures the main reason why instanton-induced processes dominate the inelastic parton-parton cross sections.

The quasielastic (QE) parton-parton scattering cross section [10] produces a cross section of order

$$\sigma_{QE} \approx \pi \rho_0^2 \kappa_0^2, \tag{1}$$

which is small in comparison to the one-gluon exchange (OGE) result at the same scale[3]

$$\sigma_{OGE} \approx \pi \rho_*^2 (\alpha_s/\pi)^2. \tag{2}$$

Below, we show that the instanton-induced parton-parton inelastic cross section is significantly enhanced,

$$\sigma \approx \pi \rho_0^2 \kappa_0, \tag{3}$$

by one power of the diluteness factor κ_0, even though it produces about $S_0 \approx 10$–15 gluons. The perturbative contributions to the inelastic cross section are suppressed. Indeed, a *one-gluon* production yields[4]

$$\sigma_{gg\to ggg} \approx \pi \rho_*^2 (\alpha_s/\pi)^3. \tag{4}$$

As a result, the instanton-induced effects dominate the perturbative contributions in the growing part of the inelastic cross section.

The distribution over the invariant mass Q of the produced gluons, deposited by the wee incoming partons onto the instanton, will be calculated in a specific unitarization model. In the weak-field limit the growth in the inelastic cross section $gg \to$ any is captured by the ''holy-grail function''

$$\sigma_{gg\to \text{any}}(Q) \approx e^{F(Q/Q_s)}, \tag{5}$$

studied in the baryon number violating processes in the standard model [12]. It peaks around the so-called sphaleron energy, which in QCD is given by the mean instanton size ρ_0,

$$E_s = Q_s/\rho_0 \approx 3\pi/(4\rho_0 \alpha_s) \approx 2 \ \text{GeV}, \tag{6}$$

for $\rho_0 \approx 1/3$ fm and $\alpha_s \approx 1/2$. Below this sphaleron energy the cross section is small but rapidly growing. As shown by Khoze and Ringwald [12], this growth can be technically attributed to a moving saddle point, reducing the relative distance between an instanton and its conjugate anti-instanton, thereby decreasing their initial action of $2S_0$. Reliable calculations can be carried out in this region. The increase in the inelastic amplitude is stopped by unitarity constraints, as suggested by Zakharov [16], precisely when the total instanton action is reduced from $2S_0$ to S_0. The specifics of the unitarization process to be discussed below will follow on the qualitative arguments suggested by Maggiore and Shifman [17]. Aside from technicalities, the physical meaning of their arguments is simple: if there is enough energy for the system to reach the top of the barrier (the sphaleron), its consecutive decay follows with unit probability. All what is needed is that the ''wee partons'' (the field of the through-moving hard partons) can encounter an instanton and deposit about 2 GeV of invariant mass. The tunneling probability at low energy on the other hand can be considered as a product of the amplitude to get *on* and *off* the barrier: hence the instanton amplitude appears twice. In QCD this enhancement of the inelastic processes with multigluon production amounts to the gain $\kappa_0^2 \to \kappa_0$ which is an enhancement by a factor of the order of 100 in the inelastic cross section relative to the quasielastic one.[5]

Although we do not use the concept of t-channel gluon exchanges (as they are summed into the eikonalized phases), some of its features remarkably survive. Already in the quasielastic process only the octet color exchange survives the high-energy limit [10]. The same feature carries over to the inelastic processes we now consider where only the octet color is transmitted from each parton line. Of course they should be in the same SU(2) subgroup to interact with a given instanton. In general, these restrictions on the possible color representations disagree with the exponentiation of multigluon production, leading to the semiclassical theory we use. In a way, this resembles the trade between using canonical as opposed to microcanonical (more accurate) ensemble in statistical mechanics. Presumably our assessment of the total cross section is still good, since the number of produced gluons is large, $N_g \approx S_0 \approx 10$–$15$.

The questions regarding the ''sphaleron decay modes'' (their decomposition into various channels) will be discussed elsewhere. We note that in recent phenomenological studies [8,7] of high-energy scattering only colorless channels (the rangs of ladders) were considered, e.g., 0^{++} (scalar glueball) and $\pi\pi$ (scalar). Although these states may contribute to the ''sphaleron decay modes,'' especially in light of the closeness of the 0^{++} mass to the sphaleron energy (6), we expect on general grounds additional contributions involving colored states as well.

Finally, we will show how the logarithmic growth in the instanton-induced parton-parton scattering amplitude takes place. Empirically, the growth is fitted at about $s \approx 100$ GeV^2. In this regime, the number of through-going effective partons can still be considered small and fixed with qqq for the nucleon and $\bar{q}q$ for mesons and photons (plus possibly some ''primordial'' glue from the QCD strings). At higher energies (although well below the Froissart bound) the power growth takes place, with possibly several effects

[3]The infrared sensitivity in OGE is cutoff by $1/\sqrt{-t} \approx \rho_*$.

[4]Both the instanton-induced and perturbative amplitudes yield $\ln s$ enhancements that are summed.

[5]The analogous electroweak instanton-induced cross section is increased by about 85 orders of magnitude due to the same enhancement, but it still remains far below any observable rate because one power of small diluteness is there.

contributing to it. The first and the simplest contribution (to be discussed in this work) is that since the elementary cross section grows, more parton-parton interaction takes place. Since the hadron size is large compared to that of the instanton $R_H^2/\rho_0^2 \approx 10 \gg 1$, we think that double, triple, etc., parton collisions will take place in a statistically independent way (Poisson). A straightforward resummation of the compounded probabilities yields a total hadronic cross section that approximately Reggeizes

$$\sigma_H(s,t) \approx \pi R_H^2 s^{\Delta(t)}, \tag{7}$$

with $\Delta(t)$ of order κ_0. In a way, we may think of $\Delta(t)$ as the square of the instanton-induced form factor. The second contribution is a re-interaction of one of the produced gluons, leading to *instanton ladders* as considered by KKL [9]. The third and final contribution may stem from rescattering through the ''primordial'' parton density at small x in the wave function itself, even at the low normalization point under consideration. These effects are not included in our ''wee'' partons which are separated in the transverse plane by a distance larger than ρ_0 from all others.

III. QUASIELASTIC SCATTERING

In this section we will recall the quasielastic results derived in Ref. [10]. This will help us streamline the notation and facilitate the comparison with the inelastic results to follow. We also discuss issues related to instantons in the weak-field limit, and show that instanton-induced processes do not discriminate between C-even and C-odd effects in the t channel, despite their multigluon structure.

A. The eikonal approximation

Using the eikonal approximation and Lehmann-Symanzik-Zimmermann (LSZ) reduction, the scattering amplitude $\mathcal{T}$ for quark-quark scattering reads [5]

$$\mathcal{T}_{AB,CD}(s,t) \approx -2is \int d^2b\, e^{iq_\perp \cdot b} \times \langle [\mathbf{W}_1(b)-\mathbf{1}]_{AC} [\mathbf{W}_2(0)-\mathbf{1}]_{BD} \rangle, \tag{8}$$

where

$$\mathbf{W}_{1,2}(b) = \mathbf{P}_c \exp\left(ig \int_{-\infty}^{+\infty} d\tau A(b+v_{1,2}\tau)\cdot v_{1,2} \right). \tag{9}$$

The two-dimensional integral in Eq. (8) is over the impact parameter b with $t=-q_\perp^2$, and the averaging is over the gauge configurations using the QCD action. AB and CD are the incoming and outgoing color and spin of the quarks.

In Euclidean geometry, the kinematics is fixed by noting that the Lorenz contraction factor translates to

$$\cosh y = \frac{1}{\sqrt{1-v^2}} = \frac{s}{2m^2} - 1 \to \cos\theta. \tag{10}$$

Scattering at high energy in Minkowski geometry follows from scattering in Euclidean geometry by analytically continuing $\theta \to -iy$ in the regime $y \approx \log(s/m^2) \gg 1$. It is sufficient to analyze the scattering for $p_1/m = (1,0,0_\perp)$, $p_2/m = (\cos\theta, -\sin\theta, 0_\perp)$, $q=(0,0,q_\perp)$, and $b=(0,0,b_\perp)$. The Minkowski scattering amplitude at high energy can be altogether continued to Euclidean geometry through

$$\mathcal{T}_{AB,CD}(\theta,q) \approx 4m^2 \sin\theta \int d^2b\, e^{iq_\perp \cdot b} \langle [\mathbf{W}(\theta,b)-\mathbf{1}]_{AC} \times [\mathbf{W}(0,0)-\mathbf{1}]_{BD} \rangle, \tag{11}$$

where

$$\mathbf{W}(b,\theta) = \mathbf{P}_c \exp\left(ig \int_\theta d\tau A(b+v\tau)\cdot v \right), \tag{12}$$

with $v=p/m$. The line integral in Eq. (12) is over a straight line sloped at an angle θ away from the vertical. Corrections to the eikonal approximation will be discussed in the next section.

B. Quasielastic amplitude

At large $\sqrt{s}$ the one-instanton contribution to the color-elastic parton-parton scattering amplitude drops as $1/\sqrt{s}$ [10]. However, the two-instanton contribution to the color inelastic part survives [10]. To set up the notation, consider the untraced and tilted Wilson line in the one-instanton background

$$\mathbf{W}(\theta,b) = \cos\alpha - i\tau\cdot\hat{n}\sin\alpha, \tag{13}$$

where

$$n^a = \mathbf{R}^{ab}\eta^b_{\mu\nu}\dot{x}_\mu (z-b)_\nu = \mathbf{R}^{ab}\mathbf{n}^b, \tag{14}$$

and $\alpha = \pi\gamma/\sqrt{\gamma^2+\rho^2}$ with

$$\gamma^2 = n\cdot n = \mathbf{n}\cdot\mathbf{n} = (z_4\sin\theta - z_3\cos\theta)^2 + (b-z_\perp)^2. \tag{15}$$

The one-instanton contribution to the scattering amplitude (11) reads

$$\mathcal{T}_{AB,CD}(\theta,q) \approx \sin\theta \int d^2b\, e^{iq_\perp\cdot b} \int dI [(\cos\alpha - 1)_{AC} - i\mathbf{R}^{a\alpha}\mathbf{n}^\alpha (\tau^a)_{AC}\sin\alpha][(\cos\underline{\alpha}-1)_{BD} - i\mathbf{R}^{b\beta}\underline{\mathbf{n}}^\beta(\tau^b)_{BD}\sin\underline{\alpha}], \tag{16}$$

where dI is short for the instanton measure

$$dI \equiv d^4z\, dn\, d\mathbf{R} \to n_0 d^4z d\mathbf{R}. \tag{17}$$

The second equality holds for fixed instanton density $n_0 = 1/\mathrm{fm}^4$ and size $\rho_0 = 1/3$ fm. The tilde parameters follow from the untilded ones by setting $\theta = \pi/2$. We note that $\underline{\tilde{\gamma}}$

$=\gamma=|\vec{z}|$. Note that only the combination **RR** survives after analytically continuing to Minkowski space and taking the large $\sqrt{s}$ limit.

The one-instanton contribution to the parton-parton scattering amplitude survives only in the color-changing channel, a situation reminiscent of one-gluon exchange [10]. As a result, the quasielastic parton-parton cross section receives a finite two-instanton contribution at large $\sqrt{s}$. The unitarized parton-parton partial differential cross section reads

$$\frac{d\sigma}{dt}\approx\frac{1}{s^2}\sum_{CD}|\mathcal{T}_{AC}^{BD}|^2, \tag{18}$$

with the averaging over the initial colors A,B understood. Simple algebra followed by the analytical continuation $\theta\rightarrow -iy$, yields [10]

$$\frac{d\sigma}{dt}\approx\frac{16n_0^2}{N_c^2(N_c^2-1)}\left|\int db\, e^{iq\cdot b}F_{ss}\left(\frac{b}{\rho_0}\right)\right|^2. \tag{19}$$

The one-instanton form factor F_{ss} is defined as

$$F_{ss}\left(\frac{b}{\rho_0}\right)=\int d^4z\,\frac{(z_\perp-b)\cdot z_\perp}{\tilde{\gamma}\underline{\tilde{\gamma}}}\sin\tilde{\alpha}\sin\underline{\tilde{\alpha}}. \tag{20}$$

In terms of Eq. (19), the quasielastic two-instanton contribution to the forward parton-parton scattering amplitude is

$$\sigma(t=0)\approx\frac{16n_0^2}{N_c^2(N_c^2-1)}\int_0^\infty dq_\perp^2\left|\int db\, e^{iq_\perp\cdot b}F_{ss}\left(\frac{b}{\rho_0}\right)\right|^2, \tag{21}$$

which is finite at large $\sqrt{s}$. Hence, for forward scattering partons in the instanton vacuum model, we expect [10]

$$\sigma_{qq}\approx\pi\rho_0^2\kappa_0^2, \tag{22}$$

which is suppressed by two powers of the density. Equation (21) is the instanton-induced generalization of the two-gluon result derived by Low [18].

C. No odderon

In the early model by Low [18] and Nussinov [19], the near-forward high-energy scattering amplitude is described by a perturbative two-gluon exchange in the t channel, which is C-parity even. Hence the qq and $\bar{q}q$ cross sections are the same to this order, a result that appears to be supported by experiment. Indeed, the difference $\sigma_{\bar{p}p}-\sigma_{pp}$ decreases at large $\sqrt{s}$ [20].

However, perturbation theory also allows for higher order corrections, e.g., SU(3) allows for a colorless combination of three gluons. Perturbatively, the odderon/Pomeron ratio is $O(\alpha_s)$ and not as suppressed as the data show. To fix this problem, a number of ideas have been put forward, some of which rely on nucleon specifics (quark-diquark structure [21]) to cancel the odderon. If that is the case, the odderon should still be observable in other hadronic reactions.

In contrast, instanton-induced processes at high energy do not suffer from the drawbacks of higher order corrections. Indeed, even though our quasielastic and even inelastic (see below) amplitudes sum up an indefinite number of gluons, switching a quark to antiquark on the external line amounts to flipping the sign of the corresponding $\sin\alpha$ contribution. As there is no interference between these and the $\cos\alpha$ terms at high energy, there is no odderon in the instanton induced amplitudes. This is easily understood by noting that an instanton is an SU(2) instead of an SU(3) field, for which the fundamental (quark) and the adjoint (antiquark) representations are equivalent.

D. Weak-field limit

In the weak-field limit, most of our results [10] simplify with interesting consequences on conventional perturbation theory. Indeed, instanton-induced amplitudes involve integration over the instanton (anti-instanton) center of mass z. So for fixed z and large impact parameter, the instanton field is weak,[6]

$$\mathbf{W}-\mathbf{1}\approx -in^a\tau^a\frac{\pi\rho_0^2}{2\gamma^2}, \tag{23}$$

which is conspicuous of a Coulomb field, familiar from perturbation theory. We now discuss the consequences of this limit on quark-quark scattering and gluon-gluon fusion to leading order.

1. $QQ\rightarrow QQ$

Inserting Eq. (23) into the quark-quark scattering amplitude yields after averaging over the global color orientations **R** to

$$\mathcal{T}_{AB,CD}\approx 2is\kappa_0\frac{\pi^2}{\tan\theta}(\tau^a)_{AC}(\tau^a)_{BD}\times\int db_\perp\, e^{iq_\perp b}\int dz_3\,dz_3'\,dz_\perp\,\frac{z_-\cdot z_+}{(z_3^2+z_-^2)(z_3'^2+z_+^2)}, \tag{24}$$

where we have defined $z_\pm=z_\perp\pm b/2$. The z integrals in Eq. (24) diverge logarithmically. This divergence is similar to the one encountered in perturbation theory [10] through the exchange of a t-channel gluon at fixed impact parameter b, i.e.,

$$\mathcal{T}(\theta,b)=\frac{2\alpha_s}{\tan\theta}\ln\left(\frac{T}{b}\right). \tag{25}$$

[6]The shift $-\mathbf{1}\rightarrow+\mathbf{1}$ amounts to a change from regular to singular gauge with no consequences for our analysis except in canceling the identity in **W**.

Hence Eq. (24) can be interpreted as the instanton-induced renormalization of the perturbative gluon-exchange result (25), with

$$2\alpha_s\left(1+2\pi^3\frac{\kappa_0}{\alpha_s}\right). \tag{26}$$

The second contribution stems from the tail of the instanton in the weak-field limit. It is natural to include this term with the perturbative one-gluon exchange, subtracting it from the truly instanton-induced amplitude. The latter is infrared finite. A similar subtraction will also be needed in the inelastic regime (see below).

2. $gg\to g$

In the weak-field limit the fusion $gg\to g$ is best analyzed in momentum space using the Fourier transform of Eq. (23),

$$A^a_\mu(k)=\frac{\pi\rho_0^2}{gk^2}\mathbf{R}^{ab}\eta^a_{\mu\nu}k_\nu. \tag{27}$$

In terms of Eq. (27) the fusion reaction in a single instanton follows from

$$\Gamma^{a1,a2,a3}_{\mu1,\mu2,\mu3}=\left(\frac{\pi\rho_0^2}{g}\right)^3(\mathbf{R}^{a1,b1}\overline{\eta}_{b1,\mu1,\nu1}k1_{\nu1})\times(\mathbf{R}^{a2,b2}\overline{\eta}_{b2,\mu2,\nu2}k2_{\nu2})(\mathbf{R}^{a3,b3}\overline{\eta}_{b3,\mu3,\nu3}k3_{\nu3}), \tag{28}$$

after using the LSZ amputated form of Eq. (27). Since $\mathbf{R}$ is isomorph to the (3,3) representation of SU(2), we note the identity

$$\mathbf{R}^{ab}\mathbf{R}^{cd}\mathbf{R}^{ef}=\frac{1}{6}\epsilon^{ace}\epsilon^{bdf}\oplus_{j=1}^{3}(2j+1,2j+1), \tag{29}$$

in terms of irreducible representations. For convenience, only the (1,1) contribution is explicitly quoted. Using Eq. (29) and the identities for the 't Hooft symbol, we obtain

$$\begin{aligned}\Gamma^{a1,a2,a3}_{\mu1,\mu2,\mu3}&(k1,k2,k3)\\ &=\left(\frac{\pi\rho_0^2}{g}\right)^3\epsilon^{a1,a2,a3}[k1\cdot k3(\delta_{\mu2,\mu3}k2_{\mu1}-\delta_{\mu1,\mu2}k2_{\mu3})\\ &+k1\cdot k2(\delta_{\mu1,\mu3}k3_{\mu2}-\delta_{\mu2,\mu3}k3_{\mu1})\\ &+k2\cdot k3(\delta_{\mu1,\mu2}k1_{\mu3}-\delta_{\mu1,\mu3}k1_{\mu2})\\ &+k1_{\mu2}k2_{\mu3}k3_{\mu1}-k1_{\mu3}k2_{\mu1}k3_{\mu2}\\ &-\epsilon_{\mu1,\alpha,\beta,\mu3}k1_\alpha k2_\beta k3_{\mu2}-\epsilon_{\mu1,\alpha,\mu2,\beta}k1_\alpha k2_{\mu3}k3_\beta\\ &-k2\cdot k3\epsilon_{\mu1,\mu2,\mu3,\alpha}k1_\alpha+\delta_{\mu2,\mu3}\epsilon_{\mu1,\alpha,\beta,\gamma}k1_\alpha k2_\beta k3_\gamma],\end{aligned} \tag{30}$$

where only the (1,1) contribution was retained. Since $k1+k2+k3=0$ only part of this expression matches kinematically the standard perturbative three-gluon vertex, thereby producing an instanton-induced contribution of relative strength κ_0/α_s^2. It can be regarded as the instanton-induced contribution to the elementary BFKL ladder. We note that the induced strength in the gluon fusion is stronger than the relative strength of κ_0/α_s seen in the exchange (26). This is a general feature of the inelastic processes as we now discuss.

IV. INELASTIC SCATTERING

To address inelastic amplitudes with instantons, the eikonal approximation has to be relaxed. To achieve that and elucidate further the character of the *s*-channel kinematics, we first derive a general result for on-shell quark propagation in a localized background field in Minkowski space. We then show how this result can be applied to instanton dynamics to analyze inelastic parton-parton scattering at high energy beyond the eikonal approximation and ladder graphs. For simplicity, all the instanton algebra will be carried out explicitly for $N_c=2$.

A. Beyond the eikonal approximation

An on-shell massless quark propagating through a localized background $A(x)$ with initial and final momenta p_1 and p_2 follows from LSZ reduction,

$$\mathcal{S}[p_1,p_2;A(x)]\equiv\langle p_2|i\vec{\not\partial}\mathbf{S}_F(x)i\vec{\not\partial}|p_1\rangle, \tag{31}$$

with $i\not\nabla\mathbf{S}_F=-1$ the background (Feynman) propagator in the instanton field. At large p_+ momentum, the quark propagates on a straight line along the light cone. This limit can be used to organize Eq. (31) in powers of $1/p_+$. The result is

$$\mathcal{S}[p_2,p_1;A(x)]=e^{i(p_2-p_1)x}\overline{u}(p_2)g\not{A}\times\sum_{n=0}^{\infty}\left(\frac{i}{2p_1\cdot\nabla}\not\nabla\frac{\not p_1\gamma_0}{2p_{10}}\not\nabla\right)^n\times\mathbf{W}_-(x_{1+},x_{1-},x_\perp)u(p_1), \tag{32}$$

where

$$\mathbf{W}_-(x_{1+},x_{1-},x_\perp)=\mathbf{P}_c\,\exp\left(-\frac{ig}{2}\int_{-\infty}^{x_{1+}}dx'_+\,A_-(x'_+,x_{1-},x_\perp)\right). \tag{33}$$

The line integral is carried along the p_1 direction of the original quark line with $x_{1\pm}=(p_0x_0\pm\vec{p}\cdot\vec{x})/p_0$. In the limit $p_{10}\to\infty$, only the $n=0$ term contributes with $x_{1\pm}=x_\pm$ being just the light-cone coordinates, thereby reproducing the eikonal result (33). The higher order terms are corrections to the eikonal-result, with the $n=1$ term accounting for both recoil and spin effects. For completeness, we also define

$$\mathbf{W}_+(x_{1+},x_{1-},x_\perp) = \mathbf{P}_c \exp\left(-\frac{ig}{2}\int_{-\infty}^{x_{1-}} dx'_- A_+(x_{1+},x'_-,x_\perp)\right). \tag{34}$$

B. Inelastic amplitude

The imaginary part of the quark-quark inelastic amplitude follows from unitarity. Schematically,

$$\mathrm{Im}\,\mathcal{T}_{if} = \mathcal{T}_{in}\sigma_{nn}\mathcal{T}^*_{nf}, \tag{35}$$

where σ_{nn} accounts for the phase space of the propagating quarks and emitted intermediate gluons. The total cross section follows then from the optical theorem $\sigma = \mathrm{Im}\,\mathcal{T}/s$. Using the result (32), we have for the total cross section in Minkowski space

$$\begin{aligned}\sigma = \frac{1}{s}\mathrm{Im}\sum_{CD}\int d[A]d[A']e^{i(S[A]-S[A'])} &\times\int\frac{d^3K_1}{(2\pi)^3}\frac{d^3K_2}{(2\pi)^3}\frac{1}{2K_{10}}\frac{1}{2K_{20}}\\ &\times\left(\sum_{n=0}^{\infty}\frac{1}{n!}\prod_{i=1}^{n}\int\frac{d^3k_i}{(2\pi)^3}\frac{1}{2k_{i0}}\mathcal{A}(k_i)\mathcal{A}'^*(k_i)\right)\\ &\times\frac{1}{VT}\int dxdydx'dy'\\ &\times e^{i(K_1-p_1)x+(K_2-p_2)y-(K_1-p_1)x'-i(K_2-p_2)y'}\\ &\times\mathcal{S}_{AC}[K_1,p_1;A(x)]\mathcal{S}^*_{AC}[K_1,p_1;A'(x')]\\ &\times\mathcal{S}_{BD}[K_2,p_2;A(y)]\mathcal{S}^*_{BD}[K_2,p_2;A'(y')].\end{aligned} \tag{36}$$

The functional integration is understood over gauge fields (to be saturated by instantons in Euclidean space after proper analytical continuation), with $\mathcal{A}(k)[\mathcal{A}'(k)]$ the Fourier transform of the pertinent asymptotic of $A(A')$ evaluated on mass shell. Similar expressions were used for sphaleron-mediated gluon fusion [12]. The difference with the present case is the occurrence of quarks in both the initial, intermediate, and final states. The sum in Eq. (36) exponentiates into the so called R term, which acts as an induced interaction between the A and A' configurations in the double functional integral (36). We will refer to it as $S(A,A')$.

The gauge fields carried inside the on-shell quark propagators $\mathcal{S}$ involve virtual exchange of background quanta with no contribution to the cut. In contrast, the on-shell gluons $\mathcal{A}(k)$ are real and the sole contributors to the cut. The $n=0$ term in Eq. (36) in the large p_+ limit reduces to the quasiinelastic contribution discussed above. The term of order n involves n-intermediate on-shell gluons plus two on-shell quarks, and contributes to the bulk of the inelastic amplitude.

The general result (36) involves no kinematical approximation regarding the in/out quark states. At high energy, all $1/p_+$ effects in Eq. (32) can be dropped to leading $\ln s$ accuracy except in the exponent. As a result, Eq. (36) simplifies dramatically:

$$\begin{aligned}\sigma\approx\frac{1}{VT}\mathrm{Im}\sum_{CD}\frac{1}{(2\pi)^6}\int dq_{1+}dq_{1\perp}dq_{2-}dq_{2\perp}&\\ \times\int[dA][dA']e^{iS(A)-iS(A')+iS(A,A')}&\\ \times\int dx_-dx_\perp dy_+dy_\perp&\\ \times e^{(i/2)q_{1+}x_- - iq_{1\perp}x_\perp+(i/2)q_{2-}y_+ - iq_{2\perp}y_\perp}&\\ \times[\mathbf{W}_-(\infty,x_-,x_\perp)-\mathbf{1}]_{AC}[\mathbf{W}_+(y_+,\infty,y_\perp)-\mathbf{1}]_{BD}&\\ \times\int dx'_-dx'_\perp dy'_+dy'_\perp&\\ \times e^{(i/2)q_{1+}x'_- - iq_{1\perp}x'_\perp+(i/2)q_{2-}y'_+ - iq_{2\perp}y'_\perp}&\\ \times[\mathbf{W}_-(\infty,x'_-,x'_\perp)-\mathbf{1}]^*_{AC}[\mathbf{W}_+(y'_+,\infty,y'_\perp)-\mathbf{1}]^*_{BD}.&\end{aligned} \tag{37}$$

Overall, the scattering amplitude follows from the imaginary part of a retarded four-point correlation function in Minkowski space. This correlation function follows from a doubling of the fields, a situation reminiscent of thermofield dynamics.

To proceed further, some dynamical approximations are needed. Let us assume that the double-functional integral in Eq. (37) involves some background field configurations characterized by a set of collective variables (still in Minkowski space), say $I=Z,\mathbf{R},\rho$, for position, color orientation, and size, respectively. Let $z=Z-Z'$ be the relative collective position. Simple shifts of integrations produce

$$e^{iQz} = e^{(i/2)q_{1+}z_- +(i/2)q_{2-}z_+ - i(q_1+q_2)_\perp z_\perp}, \tag{38}$$

with no dependence on Z,Z' in the $\mathbf{W}$'s. The integration over the location of the c.m. $(Z+Z')/2$ produces VT which cancels the $1/VT$ in front, due to overall translational invariance. The integration over the relative coordinate z produces a function of the invariant $Q^2=q_{1+}q_{2-}-(q_1+q_2)^2_\perp$ because of Lorentz invariance. With this observation and to leading logarithm accuracy, we may rewrite Eq. (37) as follows:

$$\begin{aligned}\sigma\approx\ln s\,\mathrm{Im}\sum_{CD}\frac{1}{(2\pi)^6}&\\ \times\int dQ^2\,dq_{1\perp}\,dq_{2\perp}\int dz\,d\dot{I}\,d\dot{I}'&\\ \times e^{iQz+iS(\dot{I})-iS(\dot{I}')+iS(\dot{I},\dot{I}',z)}&\\ \times\int dx_-\,dx_\perp\,dy_+\,dy_\perp\,e^{-iq_{1\perp}x_\perp - iq_{2\perp}y_\perp}&\\ \times[\mathbf{W}_-(\infty,x_-,x_\perp)-\mathbf{1}]_{AC}[\mathbf{W}_+(y_+,\infty,y_\perp)-\mathbf{1}]_{BD}&\end{aligned}$$

$$\times \int dx'_- \, dx'_\perp \, dy'_+ \, dy'_\perp \, e^{-iq_{1\perp}x'_\perp - iq_{2\perp}y'_\perp}$$
$$\times [\mathbf{W}_-(\infty, x'_-, x'_\perp) - \mathbf{1}]^*_{AC} [\mathbf{W}_+(y'_+, \infty, y'_\perp) - \mathbf{1}]^*_{BD}. \quad (39)$$

Note that the omitted exponents $e^{(i/2)q_+x_-}$, etc., are subleading in leading logarithm accuracy. The dotted integrations no longer involve the collective variables Z, Z'. The only left dependence on the relative variable z resides in the induced R term. The appearance of $\ln s$ underlines the fact that the integrand in Eq. (39) involves only Q^2 which is the transferred mass in the inelastic half of the forward amplitude, and $q_{1,2\perp}$ which are the transferred momenta through the quark form factors.

All kinematical approximations in this section were carried out in Minkowski space, a point stressed in our earlier work [10]. The result is Eq. (39) to leading logarithm accuracy. This is one of our main results, showing that the inelastic contributions to the forward quark-quark scattering amplitude cause the latter to rise with $\ln s$, irrespective of the background field used. The outcome (39) is now ripe for an analysis in Euclidean space using lattice Monte Carlo simulations or instantons as we now discuss.

C. Instanton–anti-instanton interaction

The general $\mathcal{W}$ correlation function made of the four $\mathbf{W}$'s in Eq. (37) for fixed kinematics $Q, q_{1\perp}, q_{2\perp}$, is best analyzed in Euclidean space, where the $\mathbf{W}$'s are defined at a rapidity θ and $Q_E^2 = -Q^2 < 0$. The dominant background configurations at $Q_E z \gg 1$ are instanton–anti-instanton configurations. Specifically,

$$\mathcal{W} \approx n_0^2 \sum_{CD} \int d^4z \, d\mathbf{R} \, d\mathbf{R}' \, e^{iQ_E z} e^{-\mathbf{S}(z, \mathbf{R}\mathbf{R}'^{-1})}$$
$$\times \int d^3x \, d^3y \, d^3x' d^3y' \, e^{-iq_{1\perp}(x-x') - iq_{2\perp}(y-y')}$$
$$\times [(\cos\alpha - 1)_{AC} - i\mathbf{R}^{a\alpha}\mathbf{n}^\alpha (\tau^a)_{AC} \sin\alpha]$$
$$\times [(\cos\underline{\alpha} - 1)_{BD} - i\mathbf{R}^{b\beta}\underline{\mathbf{n}}^\beta (\tau^b)_{BD} \sin\underline{\alpha}]$$
$$\times [(\cos\alpha' - 1)_{AC} + i\mathbf{R}'^{a'\alpha'}\mathbf{n}'^{\alpha'} (\tau^{a'})^*_{AC} \sin\alpha']$$
$$\times [(\cos\underline{\alpha'} - 1)_{BD} + i\mathbf{R}'^{b'\beta'}\underline{\mathbf{n}}'^{\beta'} \tau^{b'*}_{BD} \sin\underline{\alpha'}], \quad (40)$$

where the variables x, x' are defined on a tilted Wilson line of angle θ with x_4, and y, y' on an untilted Wilson line running along y_4. The instanton–anti-instanton interaction is known precisely in leading order,

$$\mathbf{S}(z, \mathbf{R}\mathbf{R}'^{-1}) = \frac{4\pi}{\alpha_s}(3u_0^2 - 1)\left(-2\frac{\rho_0^2}{z^4} + 8\frac{\rho_0^6}{z^6} + \cdots \right), \quad (41)$$

with $u_0 = \mathrm{Tr}\, U/2$ and the unitary parametrization of the orthogonal matrices

$$(\mathbf{R}\mathbf{R}'^{-1})^{\alpha\beta} = \frac{1}{2}\mathrm{Tr}(U\tau^\alpha U^\dagger \tau^\beta). \quad (42)$$

The first contribution in Eq. (41) is the well-known dipole contribution, which is known to match exactly the R contribution stemming from the exponentiation of retarded gluons from instanton vertices [12].

There are many contributions in Eq. (40). However, we note that in Minkowski space, the dominant contribution while continuing in θ involves **RRRR**. From here on, it will be the only one retained. With this in mind, we carry first the integration over the collective variable $\mathbf{R}$ and $\mathbf{R}'$ in the SU(2) case by explicitly carrying part of the group integration. Setting $u_0 = \cos\chi$, and averaging over SU(2) gives

$$\mathbf{RRRR} = +\frac{2}{\pi} I_1 \mathbf{n}\cdot\mathbf{n}'\underline{\mathbf{n}}\cdot\underline{\mathbf{n}}' + \frac{2}{3\pi} I_2 [-2\mathbf{n}\cdot\mathbf{n}'\underline{\mathbf{n}}\cdot\underline{\mathbf{n}}'$$
$$+ 4(\mathbf{n}\cdot\underline{\mathbf{n}}\mathbf{n}'\cdot\underline{\mathbf{n}}' - \mathbf{n}\cdot\underline{\mathbf{n}}'\mathbf{n}'\cdot\underline{\mathbf{n}})]$$
$$+ \frac{2}{15\pi} I_3 [-\mathbf{n}\cdot\mathbf{n}'\underline{\mathbf{n}}\cdot\underline{\mathbf{n}}' + 4(\mathbf{n}\cdot\underline{\mathbf{n}}\mathbf{n}'\cdot\underline{\mathbf{n}}'$$
$$+ \mathbf{n}\cdot\underline{\mathbf{n}}'\mathbf{n}'\cdot\underline{\mathbf{n}})], \quad (43)$$

with

$$I_k = \int_0^\pi d\chi \sin^{2k}\chi \cos^{6-2k}\chi e^{-\mathbf{S}(z, \cos^2\chi)} \quad (44)$$

for $k = 1,2,3$. Inserting Eq. (44) back into Eq. (40) and performing the analytical continuation back to Minkowski space shows that only the combination

$$(\mathbf{n}\cdot\underline{\mathbf{n}}\mathbf{n}'\cdot\underline{\mathbf{n}}' + \mathbf{n}\cdot\underline{\mathbf{n}}'\mathbf{n}'\cdot\underline{\mathbf{n}}),$$

survives. The result is

$$\mathcal{W}(Q, q_{1\perp}, q_{2\perp}) = (16\pi^5)^{1/2}\mathbf{K}(q_{1\perp}, q_{2\perp})\mathrm{Im}\, n_0^2$$
$$\times \int_0^\infty dR \left(\frac{R}{Q}\right)^{3/2} \int_0^\pi d\chi \sin^6\chi$$
$$\times e^{QR - \mathbf{S}(R, \cos^2\chi)}, \quad (45)$$

with the induced kernel

$$\mathbf{K}(q_{1\perp}, q_{2\perp}) = |\mathbf{J}(q_{1\perp})\cdot\mathbf{J}(q_{2\perp}) + \mathbf{J}(q_{1\perp})\times\mathbf{J}(q_{2\perp})|^2. \quad (46)$$

We have introduced our generic instanton-induced form factor

$$\mathbf{J}(q_\perp) = \int dx_3 \, dx_\perp \, e^{-iq_\perp x} \frac{x_\perp}{|x|} \sin\left(\frac{\pi|x|}{\sqrt{x^2 + \rho_0^2}} \right), \quad (47)$$

which is purely imaginary,

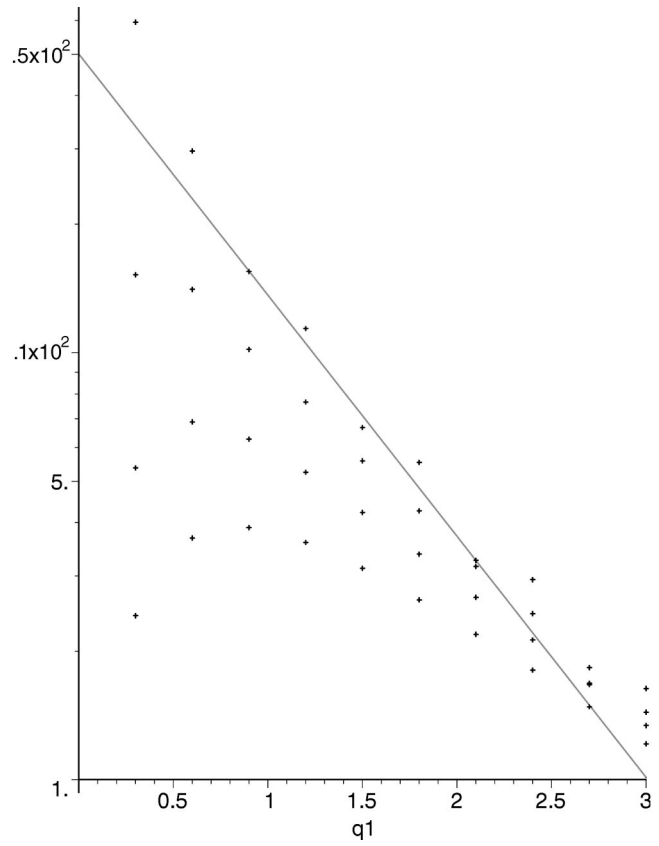

FIG. 2. The induced instanton form factor $|\mathbf{J}(q_\perp)|$ (points) and its parametrization (49) (solid line) versus $q1=q_\perp\rho_0$. The four sets of points (counting from top to bottom) correspond to different parametrizations of the instanton shape (see Sec. V C below) **a** $=0,0.25,0.50,0.75$ (top to bottom).

$$\mathbf{J}(q_\perp)=-i\frac{\hat{q}_\perp}{\sqrt{q_\perp}}\int_0^\infty dx\, J_{3/2}(q_\perp x)\left[(2\pi x)^{3/2}\sin\left(\frac{\pi|x|}{\sqrt{x^2+\rho_0^2}}\right)\right]. \tag{48}$$

Here $J_{3/2}$ is a half-integer Bessel function. In the weak-field limit the instanton contributes a term ${}^3\sqrt{x}/x^2\approx 1/\sqrt{x}$ that causes the instanton-induced form factor to diverge. This divergence is analogous to the one encountered in $QQ\to QQ$. The behavior of Eq. (48) is shown in Fig. 2 (top points). Apart from the unphysical (perturbative) singularity at small $q_\perp$, the instanton-induced form factor can be parametrized by a simple exponential

$$\mathbf{J}(q_\perp)\approx -i\hat{q}_\perp 50e^{-1.3q_\perp\rho_0}, \tag{49}$$

which is the solid line shown in Fig. 2. We note that this is very different from just the Fourier transform of the instanton field used as a form factor in Ref. [9] (see further discussion in Sec. VI B below). Throughout, the tail of the instanton will be subtracted resulting into a renormalization of the perturbative result.

The imaginary part of Eq. (47) is readily assessed in the dipole approximation by retaining only the first contribution in Eq. (41). Carrying the R and γ integrations by saddle point we obtain a purely imaginary result to leading order owing to the unstable mode around the instanton–anti-instanton configuration. The result for the total cross section is

$$\sigma\approx\pi\rho_0^2\kappa_0^2\ln s\,\frac{64}{15}\,\frac{1}{(2\pi)^8}\times\int dq_{1\perp}\,dq_{2\perp}\mathbf{K}(q_{1\perp},q_{2\perp})\,\mathrm{Im}\,i\mathbf{C}\alpha^{3/10}\times\int_{(q_1+q_2)_\perp^2}^\infty dQ^2\,\frac{e^{(5/2)(2\pi Q^4/\alpha)^{1/5}}}{Q^{37/10}}, \tag{50}$$

with $\mathbf{C}$ a number inherited from the R and χ saddle points,

$$\mathbf{C}=10\sqrt{6}(2\pi)^{1/5}\left(\frac{16\pi}{3}\right)^3. \tag{51}$$

All the integrations are over dimensionless variables re-expressed in units of the instanton size ρ_0. From here on, this will be assumed unless indicated otherwise. The Q integration diverges at the upper end. This is not surprising since the dipole approximation is valid for small invariant mass Q^2 or large separation z. As Q^2 increases, the higher order contributions in Eq. (41) become important. This is the realm of the streamline as we now discuss.

D. Streamline

In the Euclidean regime $Q_E z\approx 1$, the instanton–anti-instanton overlaps as their interaction becomes strong. In this case, it is more appropriate to use the streamline configuration, which is a gauge configuration that interpolates between an instanton–anti-instanton asymptotically and the vacuum, following the path of least action (valley). A very good parametrization of the streamline follows from conformal symmetry. In particular,

$$\mathbf{S}(z,\cos^2\chi)=a(z)+b(z)\cos^2\chi+c(z)\cos^4\chi, \tag{52}$$

where $a(z)$, $b(z)$, and $c(z)$ are known functions of z [14]. Using Eq. (52) in the saddle point approximation carried above allows for a better assessment of the Q^2 integrand in Eq. (50). In particular,

$$\mathbf{C}\alpha^{3/10}\frac{e^{(5/2)(2\pi Q^4/\alpha)^{1/5}}}{Q^{37/10}}\to B(Q)=e^{F(Q/Q_s)}, \tag{53}$$

where Q_s^2 is the sphaleron invariant mass squared. The streamline configuration allows us to extend the validity of the dipole approximation to higher Q^2, through the holy-grail function F. The specific form of F will not be needed if unitarization takes place as we now show.

E. Multi-instantons and unitarization

The inelastic contributions to the quark-quark scattering amplitude causes the total cross section to grow rapidly with the longitudinal energy transferred Q^2. Since the streamline configuration leads eventually to the vacuum, one may be

tempted to argue that this generates unsuppressed multigluon production with unbounded cross section [16]. This conclusion is physically incorrect.

Indeed, in the analogous problem of baryon number violation in the standard model, Zakharov [16] has argued that for $Q \approx Q_s$ the rise in the cross section has to stop because of unitarity constraints. Maggiore and Shifman [17] suggested that as Q^2 increases, or equivalently as the instanton–anti-instanton separation decreases, multi-instanton effects become important. Unitarization can be simply enforced by resumming a chain of alternating instanton–anti-instanton configurations, leading to a unitarized amplitude confirming Zakharov's observations.

Following the Maggiore and Shifman suggestion in the baryon number violation problem, we perform the large Q^2 integration in Eq. (50) using iterated multi-instanton contributions. This is similar to (although different from) the usual treatment of resonances, when the attractive interaction is iterated and leads to a Breit-Wigner result. Specifically, the imaginary part in Eq. (50) now reads

$$\sum_{n=1}^{\infty} \kappa_0 (\kappa_0 iB(Q))^n, \tag{54}$$

for alternating insertions of instantons and anti-instantons (chain). Each factor of iB results from the insertion of an extra instanton or anti-instanton on the chain, producing a bond with an extra unstable mode. Hence the total cross section is

$$\sigma \approx \pi \rho_0^2 \ln s \frac{64}{15} \frac{1}{(2\pi)^8} \times \int dq_{1\perp}\, dq_{2\perp}\, \mathbf{K}(q_{1\perp}, q_{2\perp}) \kappa_0 \times \int_{(q_1+q_2)_\perp^2}^{\infty} dQ^2 \frac{\kappa_0 B(Q)}{1+\kappa_0^2 B(Q)^2}. \tag{55}$$

The integrand in Eq. (55) rises with $B(Q)$ as expected in the small Q regime and falls off as $1/B(Q)$ due to unitarization. The dominant contribution takes place at the sphaleron invariant mass

$$B(Q_s) \approx 1/\kappa_0 \tag{56}$$

for which the total cross section (41) becomes

$$\sigma \approx \pi \rho_0^2 \ln s \kappa_0 \frac{64}{15} \frac{1}{(2\pi)^8} \int dq_{1\perp}\, dq_{2\perp}\, \mathbf{K}(q_{1\perp}, q_{2\perp}). \tag{57}$$

Note that under the condition (56) the Q^2 integration amounts to a number of order 1, a measure of the area under the curve peaked at Q_s with maximum 1/2 and width of order 1. The rise in the partial inelastic cross section due to multi-instanton effects results in an increase of the cross section by one power of the diluteness factor which is about a 100-fold increase. The inelastic cross section grows logarithmically with s, in contrast to our original quasielastic estimate [10].

The energy following from Eq. (56) implies that half of the original instanton–anti-instanton action of $2\times(8\pi^2/g^2)$ is compensated by their attraction. In other words, the s exchange in the inelastic process starting from the vacuum is *half instanton*. This is the transition from vacuum to a static QCD sphaleron. This leads us to the following important observation: at high energy, the inelastic s-channel contributions to parton-parton scattering in leading logarithm approximation are QCD sphalerons.

V. SOFT POMERON FROM INSTANTONS

In this section we will show that in the semiclassical analysis the parton-parton cross section increases at most as $\ln s$, while the hadron-hadron cross section as a polynomial in $\ln s$, with a degree fixed by the number of hard collisions in the transverse plane.

A. Intercept

In this paper we have only calculated the growing part of the qq cross section: in order to relate it to hadron-hadron scattering some phenomenology has to be done. We defer some discussion of how to do it to Sec. VII B below, and now proceed with the extremely naive *additive quark* model, from the 1960s, which ignores the gluons and sea quarks, and consider a nucleon as a set of three constituent quarks. The total quark-quark cross section can then be assessed in the following way. Using cross section at $\sqrt{s}<30$ GeV, where it does not grow yet, we write

$$\sigma_{qq} = \frac{1}{9}\sigma_{pp} \approx 3.3 \text{ mb}. \tag{58}$$

Setting $\sigma_{qq} = \pi r_0^2$ we find that Eq. (58) reflects on a typical scattering disk of radius $r_0 \approx 1/3$ fm.

The instanton contribution to the inelastic process yields a logarithmically growing cross section

$$\sigma(s,t) \approx \pi \rho_0^2 (\#\kappa_0 \ln s + \cdots). \tag{59}$$

Hence

$$\sigma(s,t) \approx \pi \rho_*^2 (\alpha_s/\pi)^2 + \pi \rho_0^2 \Delta(t) \ln s \tag{60}$$

with

$$\Delta(0) = \kappa_0 \frac{64}{15} \frac{1}{(2\pi)^8} \int dq_{1\perp}\, dq_{2\perp}\, \mathbf{K}(q_{1\perp}, q_{2\perp}). \tag{61}$$

Using Eq. (46) we note that the spin-0 and spin-1 parts contribute equally to the intercept, giving

$$\Delta(0) = \kappa_0 \frac{64}{15} \frac{1}{(2\pi)^8} \left(\int_0^{\infty} dq\, \mathbf{G}^2(q) \right)^2, \tag{62}$$

where we have defined the scalar form factor $\mathbf{G}$ as

$$\mathbf{J}(q) = -i\frac{\hat{q}}{\sqrt{q}}\frac{\mathbf{G}(q)}{\sqrt{2\pi}}. \tag{63}$$

A numerical estimate of Eq. (62) can be made using the parametrization (49) which removes the unphysical singularity at $q_\perp = 0$. The result is

$$\Delta(0) = 9.48\kappa_0 \approx 0.12, \tag{64}$$

which is close to the phenomenological intercept of 0.093 [22] for the soft Pomeron. Since the instanton density is known within a factor 2, this result should be regarded as an estimate. Additional effects absent in the present instanton estimate will be discussed below. Our main conclusion is that the smallness of the soft Pomeron intercept directly reflects on the diluteness of the instantons in the QCD vacuum, thereby providing us with a first hand empirical glimpse to this important parameter.

B. Slope

The t dependence in the parton-parton cross section follows from the inelastic processes with net momentum flow in the t channel. We can change minimally the forward scattering amplitude to allow for this, leading to the following expression:

$$\Delta(t) = \kappa_0 \frac{64}{15}\frac{1}{(2\pi)^8}\int dq_{1\perp}\, dq_{2\perp}\, \mathbf{H}(q_{1\perp}, q_{2\perp}; t), \tag{65}$$

with the new t-dependent induced kernel ($t = -q_\perp^2$)

$$\begin{aligned}\mathbf{H}(q_{1\perp}, q_{2\perp}; t) \equiv & [\mathbf{J}(q_{1\perp} - q_\perp/2)\cdot\mathbf{J}(q_{2\perp} - q_\perp/2) \\ & + \mathbf{J}(q_{1\perp} - q_\perp/2)\times\mathbf{J}(q_{2\perp} - q_\perp/2)] \\ & \times[\mathbf{J}(q_{1\perp} + q_\perp/2)\cdot\mathbf{J}(q_{2\perp} + q_\perp/2) \\ & + \mathbf{J}(q_{1\perp} + q_\perp/2)\times\mathbf{J}(q_{2\perp} + q_\perp/2)]^*.\end{aligned} \tag{66}$$

The form factors are defined as in Eqs. (47) and (48). For $t \approx 0$, we have $\Delta(t) \approx \Delta(0) + t\Delta'(0)$. The slope parameter $\Delta'(0)$ follows from a Taylor expansion of Eq. (65) *after* integration. Using Eq. (49) which removes the unphysical singularity at $q_\perp \approx 0$ (related to the perturbative singularity discussed earlier in $QQ \to QQ$ scattering), we can perform the double integrations in Eq. (65) to obtain $\mathbf{H}(q_\perp^2)$ as shown in Fig. 3. Modulo the prefactors in Eq. (65) this is just the Pomeron trajectory for $t < 0$ (physical region). The upper curve refers to instantons with unmodified vacuum sizes ($\mathbf{a} = 0$), while the lower curve corresponds to slightly smaller instantons ($\mathbf{a} = 0.25$). The trajectory never crosses zero, implying that the cross section grows in the physical region with increasing $\sqrt{-t}$.

We note that the trajectories decrease rapidly with increasing $\sqrt{-t}$, showing that most of the variation is located around 0. The induced trajectories are sensitive to the instanton size through a rescaling of the induced form factor by the parameter **a**. Indeed, the slope $\Delta'(0)$ relates to the Pomeron slope through

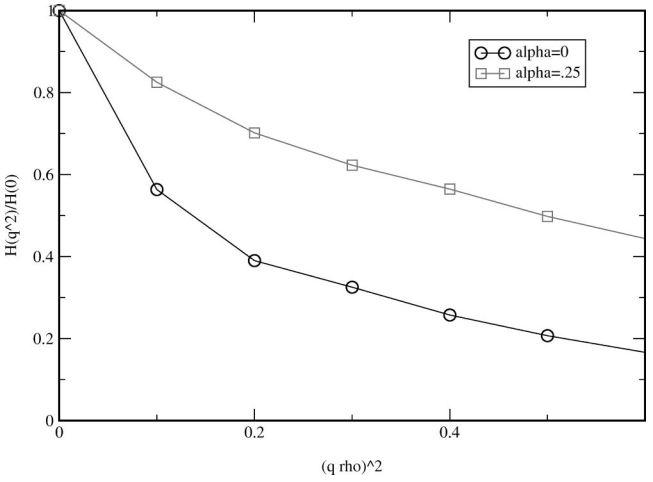

FIG. 3. Instanton-induced form factor $\mathbf{H}(q_\perp^2)$ at the origin of the soft Pomeron trajectory, normalized to its value at $t = 0$, versus $-t\rho_0^2 = q_\perp^2\rho_0^2$. The squares refer to the unmodified instanton shape and the circles to the modified one.

$$\Delta'(0) = \alpha' = (2 - -0.8)/\mathrm{GeV}^2, \tag{67}$$

with 2 corresponding to the unmodified instanton-induced form factor ($\mathbf{a} = 0$) and 0.8 corresponding to a scaled down instanton-induced form factor ($\mathbf{a} = 0.25$).

Our main point is that the smallness of the soft Pomeron intercept α' reflects directly on the smallness of the squared instanton radius. Our trajectory curves are similar to those reported by KKL [9] (who also continued their trajectories to the unphysical region $t > 0$). However, this comparison is only qualitative, since the induced form factor used in KKL differs fundamentally from the one we have derived (see discussion below). The issue of the size dependence was not addressed in Ref. [9].

C. Instanton shape dependence

An ensemble of instantons in the QCD vacuum is always described by retaining the instanton configurations in the *singular* gauge, where the topological singularity is located at the instanton center.[7] In the singular gauge, the instanton gauge field falls off as $A \approx \rho_0^2/x^3$ at large x, providing a ground for a dilute analysis. By keeping the topological properties at the center, a modification of the ''tail'' of the gauge field at large distances may be allowed. Moreover, since the semiclassical analysis holds only for strong fields, these tail modifications are in general expected.

There are many effects which can modify the tail of the instantons, an example is through interactions. Indeed an

[7]This is in contrast with the regular gauge where the singularity is removed to the sphere at infinity. Some subtleties regarding this transformation are discussed in Ref. [23].

early variational estimate of the instanton vacuum energy using exponentially modified instanton form factors such as $e^{-\mathbf{a}x/\rho_0}$ [24] shows a minimum at $\mathbf{a}\approx 0.5$. Other possible reasons for instanton-shape modifications can be due to confinement as discussed in the context of the QCD dual superconductor [25]. Lattice studies of various gluonic correlators also show rapid exponential falloff. Thinking about the lowest glueballs, with their 2-GeV mass scales as a two-gluon bound state, may imply an even larger sizing down with $\mathbf{a}\approx 1$.

Most previous applications of instanton physics in QCD were found to be generally insensitive to shape variations. Indeed, those related to light quarks are based on the fermionic zero modes, which exist and are normalized independently of the tail of the instanton field. Also, the correlators of the scalar field strength combination $G^2_{\mu\nu}$ [26] are instanton-shape insensitive since they fall off rapidly at large x (as $1/x^8$ in perturbation theory). The only exception which has been studied before [29] is the correlator of the *first* powers of the field strength (naturally, connected by transpoters to make it gauge invariant): this correlator has been calculated for a range of modification parameters, shown to be sensitive to it, and also compared to lattice data available. General agreement is seen at nonzero but *modest* modification of the shape: nevertheless, no unique suggestion on what is the most appropriate magnitude of the modification has been made.

We found, however, that in the present problem the issue of the instanton shape is actually very important. Without modifiction the induced form factors fall off as $1/x^2_\perp$ and their integrated effect in the transverse plane (through $dx_\perp$) diverges logarithmically. This diveregence can be removed by any modification.

Therefore the instanton-shape modifications cause our results (intercept and slope) to change quantitatively, showing the limitations in the present analysis. To illustrate this, consider changing the description from regular to singular gauge and inserting the exponential modifications in the instanton tails. Hence the argument in the definition of the induced instanton form factor **J** changes accordingly,

$$\frac{\pi|x|}{\sqrt{x^2+\rho_0^2}} \to \pi\left(\frac{|x|}{\sqrt{x^2+\rho_0^2}}-1\right)e^{-\mathbf{a}|x|/\rho_0}. \tag{68}$$

The effect on the form factor **J** is illustrated in Fig. 2. In the unmodified case with $\mathbf{a}=0$ (top points) the form factor rises towards small momentum transfer, which is not the case for $\mathbf{a}>0$. As expected the modifications due to **a** are small at large $q^2_\perp$.

D. Reggeization and shadowing

Unlike what is done in conventional soft Pomeron phenomenology, we are not trying in this work to unite both the nongrowing and growing part of the cross section into one common Regge pole, the Pomeron. Although the point of view taken in this work ascribes those two effects to rather different physical processes, the color exchanges and prompt production of some colored clusters of nonperturbative field, the t channel iteration of both effects may still create a common pole. However, we think that any meaningful discussion of it can only be made provided that there is sufficient understanding of dynamics of *both* components of the amplitude.

The issue of multiple instanton-induced interactions in s channel can in principle be addressed. Since hadrons are composed of several partons, each capable of a collision with another one being close in the transverse plane. Even with only three quarks in a nucleon, we may have up to $3\times 3=9$ possible subcollisions in the NN case. With appropriate normalization point $Q\sim 1$ GeV we have several gluons as well, and at very high energies their number is expected to grow further. Since the hadron diffractive size R_H ($R_H\approx 3r_0\approx 1$ fm) is large (and logarithmically expanding) in comparison to the interaction range, the maximum number of independent collisions can be as large as $N_*\approx R_H^2/\rho_0^2\approx 10$.

On the other hand, the probability of multiple instanton-induced collisions is proportional to higher power of the instanton density, thereby small. Empirically, the fits to the rising part of the cross section, i.e., higher powers of $\ln^n(s/s_0)$ with $n>1$ are still rather uncertain. A simple probabilistic treatment may consider pair collisions as statistically independent, with a Poisson distribution. As a result, the resummed contribution to the total hadron-hadron cross section σ_{HH} reads

$$\sigma_{HH}(s,t)\approx \pi R_H^2\sum_{n=1}^{N_*}\frac{1}{n!}\left(\frac{\sigma(s,t)}{\pi\rho_0^2}\right)^n, \tag{69}$$

which is a polynomial in $\ln s$ of degree $N_*\approx 10$. Since Eq. (69) is a polynomial in $\kappa_0\approx 0.01$ as well, the expansion is well approximated by its first two terms within the Froissart bound. By considering N_* to be infinite, the answer looks like a Reggeized cross section ($\rho_*\approx\rho_0$)

$$\sigma_{HH}(s,t)\approx \pi R_H^2(e^{\alpha_s/\pi}s^{\Delta(t)}-1), \tag{70}$$

with an asymptote $s^{\Delta(t)}$ fixed by the instanton density.

However, this naive probabalistic treatment ignores screening (shadowing) corrections, which also are of higher orders in density but enter the total cross section with alternating signs. When the total probability of all interactions at given impact parameter becomes close to 1, unitarity precludes any further growth in the cross section, and screening becomes dominant. Generally, the interference between higher order processes depends on the quark correlation in the transverse plane which is poorly known so far, and eventually given by some pertinent light-cone wave functions.

We hope to discuss higher order effects elsewhere, and now proceed to compare our analysis and results to those of other recent works, as well as discuss their other limitations.

VI. WEAK-FIELD APPROXIMATION

In this section we will provide some qualitative arguments regarding the relationship between the semiclassical analysis carried above and the weak-field approximation used in previous analyses, e.g., in KKL [9].

A. Weizsacker-Williams approximation

Consider that each hard parton is surrounded by a cloud of wee partons making a virtual Coulomb field in its rest frame. A hard parton with large rapidity y (not to be confused with a y-coordinate in this section) going through a classical field, radiates quasireal gluons

$$Q(p)\to Q(k)+g^*(q) \tag{71}$$

with a Weizsacker-Williams distribution

$$dN_{WW}\approx \frac{\alpha_s}{\pi}\frac{d\omega}{\omega}\frac{dq_\perp^2}{q_\perp^2}\mathbf{F}_E^2(q_\perp^2), \tag{72}$$

for fixed energy $\omega=q_0$ and transverse momentum. Terms of order $\omega/\sqrt{s}$ and $q_\perp^2/s$ have been ignored. $\mathbf{F}_E$ is the color-electric Sachs form factor of the hard parton induced by the classical field, which is 1 for a point charge.

Hard parton-parton scattering in the Weizsacker-Williams approximation follows in two stages:

$$\begin{aligned} Q(p_1)+Q(p_2)\to Q(k_1)+Q(k_2)\\ +[g^*(q_1)+g^*(q_2)\to \mathbf{X}(q_1+q_2)], \end{aligned} \tag{73}$$

from which the inelastic cross section follows by convoluting the entrance fluxes (71) with the gluon-gluon fusion cross section. Setting $dy=d\omega/\omega$ we have

$$\begin{aligned} d\sigma\approx\left(\frac{\alpha_s}{\pi}\right)^2\frac{dq_{1\perp}^2}{q_{1\perp}^2}\frac{dq_{2\perp}^2}{q_{2\perp}^2}dy_1\,dy_2\,\mathbf{F}_E^2(q_{1\perp}^2)\\ \times\mathbf{F}_E^2(q_{2\perp}^2)\sigma_{gg}(q_{1\perp}-q_{2\perp},y_1-y_2). \end{aligned} \tag{74}$$

The total fusion cross section sums over all the exclusive cross sections in Eq. (73). In particular, it depends only on the rapidity difference (the energy of the gg subprocess) and the transferred transverse momentum. Thus one can integrate over the c.m. rapidity $Y=(y_1+y_2)/2$, which is bracketed by the rapidity of the original hard partons, leading to the standard $\ln s$ enhancement. The logarithmic rise in the inelastic cross section is just a measure of the available longitudinal phase space of the produced subsystem. The magnitude of the rise depends on the exclusive cross section $\sigma_{gg\to\mathbf{X}}$ summed over all final states $\mathbf{X}$, and the induced form factors that we now discuss.

B. Induced form factors

The instanton-induced form factors are important elements of the high-energy scattering calculations we have described. They make all transfer integrations finite, thereby determining the magnitude of the cross section. They also keep the instanton effects from being part of the hard processes. In a recent investigation by KKL [9], the instanton-induced form factor (now in absolute units)

$$\mathbf{F}_E(q_\perp^2)\approx\frac{1}{(q_\perp\rho_0)^4}\left(1-\frac{1}{2}(q_\perp\rho_0)^2K_2(q_\perp\rho_0)\right), \tag{75}$$

was derived using the weak-field limit. Equation (75) is simply the Fourier transform of the instanton field (27). The weak-field approximation is justified if only a single-gluon exchange between the through-going parton and the instanton is registered. The single-gluon approximation and the Weizsacker-Williams approximation are justified when the parton impact parameter exceeds the instanton size ρ_0, which is equivalent to $q_\perp\rho_0\ll 1$. But in this case, the form factor (75) reduces to 1.

In general, the parton-instanton interaction takes place when the incoming parton punches through the instanton at an impact parameter comparable to the instanton size ρ_0, for which $q_\perp\rho_0\leqslant 1$. Hence we cannot use the weak-field approximation and the induced form factors are given by Wilson lines,

$$\mathbf{F}_E(q_\perp^2)\approx\int\frac{d^3x}{\rho_0^3}e^{iq_\perp\cdot x}[\mathbf{W}(\infty,x_\perp,x_3)-\mathbf{1}], \tag{76}$$

with open color indices (see above). Our induced form factors resum multiple gluon exchanges, while those discussed by KKL [9] do not.

VII. ADDITIONAL DIFFRACTIVE CONTRIBUTIONS

Throughout two semiclassical resummations were used: (i) the eikonalized phases which resum multiple interaction with the through-going partons, and (ii) the produced gluons which resum into an instanton–anti-instanton interaction. In this section, we discuss additional effects that we have not retained.

A. Interference and interaction

The diagrams shown in Fig. 4 describe additional interference (a) and interaction (b) effects between the gluonic radiation from the hard partons and the instanton, which we have not considered in our analysis. The interference of the radiation (a) with the instantons can be argued to be small, for the following reason. Kinematically the radiation from the external line has a flat rapidity distribution extending all the way to the rapidity of the hard parton (see the Weizsacker-Williams approximation), while instantons produce about $S_0\approx 10$–15 gluons within a cluster occupying one unit in rapidity space. The overlap between the radiation and the 10–15 gluons is about $1/\ln s$ thereby compensating the logarithmic growth in the cross section.

A possible way to include the radiation effects is to calculate the eikonal factors $\mathbf{W}$ in the *combined* field of an instanton–anti-instanton in the simplest sum ansatz. The interaction diagrams (b) can then be viewed as additional corrections to this simple ansatz, diagrammatically describing a more appropriate solution. Since no analytical formulas for path-order exponents in a field more complicated than that of a single instanton is available, inclusion of those corrections

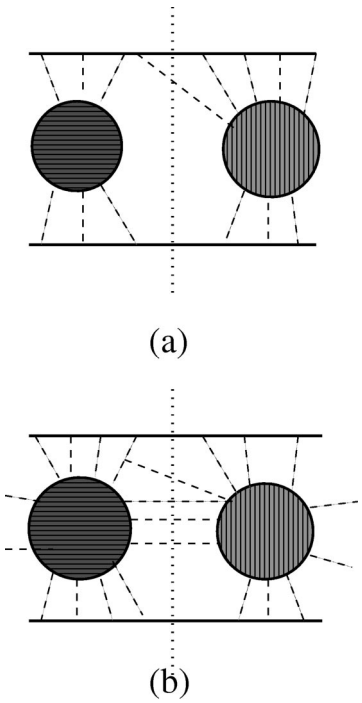

FIG. 4. The interference (a) and interaction (b) diagrams not included in our analysis.

would complicate the present analysis considerably. We hope to report on these effects elsewhere.

B. Additional partons

As we did emphasize at the beginning of this paper, our analysis of the collision processes is based on the parton model, whereby the parton-parton cross sections (evaluated) are separated from the hadronic wave functions (not evaluated). The separation depends on what is exactly meant by our distinction of a parton from through-going quark, which is of course scale dependent. In our case, the separation scale is set by the mean instanton size $\rho_0 \approx 1/(600\ \mathrm{MeV}) \approx 1/3$ fm. This choice may appear to be in contradiction with the usual statement that perturbative QCD cannot be used below the scale of 1 GeV. However, there is no contradiction if those deviations from perturbative QCD are precisely due to the instanton effects we account for. For phenomenological and theoretical arguments in favor of this viewpoint in the vacuum we refer to Refs. [3] and [27]. Our present analysis extends these arguments to diffractive scattering. Although we have ignored perturbative gluons and field-theoretical renormalizations of all quantities discussed, we believe they have to be included around our semiclassical treatment for our results to be complete.

At the low normalization scale of order 0.6 GeV the partons are dressed by their surrounding fields, perturbative and nonperturbative, and for all purposes are effective objects. We have referred above to the nucleon as being made of three quarks, the photon of a quark-antiquark, etc. However, experiments have shown that even at this low scale not *all* glue (and the sea quarks and antiquarks) reside inside effective quarks. The simplest part of the gluons are perturbative ''wee'' partons, which in fact were included above, in our **W** factors. The experimental data from HERA show that at such low normalization point the gluonic density is very different from what one finds at larger scales: it does not rise toward small x but rather stays about flat, or even decreases.

But still not all glue of the nucleon is perturbative. Indeed, in the simplest constituent quark model for hadron spectroscopy the effective wave function for $\bar{q}q$ and qqq still requires the help of a confining potential, or a QCD string.

All this suggests that a quantitative approach should include also the place for through-going gluons inside the high-energy nucleon or photon,[8] for which the instanton-induced cross section has not been assessed yet. There is no technical difficulty to do so along the lines we have presented, and we expect their cross section to be generally larger, improving the agreement between our theoretical prediction and empirical rate of the cross section growth. Furthermore, as the gluon contribution roughly scales as as Casimir operators, we expect qg and then gg cross section to be about 4 and 16 times larger than qq ones, and thus be comparable to quark scattering even if the nonperturbative glue at such low normalization point is relatively small.

VIII. CONCLUSIONS AND OUTLOOK

In this work we have extended our evaluation of the instanton contribution to the scattering of partons at large $\sqrt{s}$ and small $-t/s$, from quasielastic to inelastic collisions. The present findings and results support previous suggestions about the importance of instantons in high-energy and near-forward scattering amplitudes in QCD. Although our analysis differs significantly from the one recently reported by KKL in Ref. [9], the underlying physics is about the same. All in all, instantons are shown to play a significant role in diffractive processes.

Throughout, we have tried to make a consistent use of purely semiclassical treatments. The interactions with the through-going partons are included in the eikonalized factors, with any number of gluons, and the inelastic production of any number of gluons is summed into an instanton–anti-instanton interaction. Both approaches have been developed previously, but their combined application to the soft Pomeron problem is new. At higher invariant masses of the produced system, we also carried out unitarity considerations (through a chain of alternating instanton and anti-instanton) in somewhat more detail than it has been done previously.

Certain general features are the same for quasielastic and inelastic instanton-induced scattering. In particular, both correspond to the relatively small (on the hadronic scale) transverse dimention scale $x_t \sim \rho \sim 1/3$ fm. Also both have the same expression for quarks and antiquarks, producing *no oderons*; this goes back to the SU(2) nature of the instanton.

Two major differences between quasielastic and inelastic processes have been found. (i) The production of an interme-

[8]In the stochastic vacuum model [28], those gluon exchanges originating from the canvassing strings are assumed to be even dominant in the hadronic cross section.

diate multigluon system leads to a $\ln s$ growth in the total cross section, opening up the possibility to explain soft Pomeron physics after pertinent resummation. (ii) The inelastic cross section is much larger, in fact it is parametrically larger by an inverse power of the instanton diluteness parameter (about a factor of 100). The Pomeron intercept is small because it is simply proportional to the *small instanton diluteness* parameter in the QCD vacuum. (iii) The Pomeron slope is small, because it is directly related to the instanton induced form factors on the eikonalized hard partons, hence to *small instanton sizes* in the QCD vacuum. (iv) For the first time in QCD applications of instantons, we have found that the instanton shape at large distances from the center can actually impact on a physical observable such as the Pomeron slope.

Our work can be extended in a number of ways. The most straightforward extension is to small size dipoles [10] and gluons as partons participating in scattering. Small size dipole scattering is related to processes with virtual photons, such as $\gamma^* h$ and $\gamma^* \gamma$ and even $\gamma^* \gamma^*$ with two virtual photons. The next set of questions which can be also addressed in the present framework relates to the nature of the produced multigluon systems in the exclusive reactions, or the ''sphaleron decay'' problem. The total cross section we evaluated can be decomposed into pertinent channels with given quantum numbers involving specific hadrons and glueballs. Since in the inelastic processes, particle production is in general masked by multiple production from string decays from the final stage, we suggest to focus on double diffractive cross sections where the produced hadrons are selected alone and separated by large rapidity gaps from the target and the projectile.

Finally, one may ask what happens at very large energies. We have briefly discussed a naive probablistic resummation of our basic process, resulting in a cross section growing as $\ln s$, but have not really considered the screening corrections of the same order. We have not addressed the issue of Reggeization due to t-channel iterations, or the instanton ladders considered in KKL [9]. Furthermore, we have not addressed very high energies: a comparison of the present results with the data will eventually tell us if there is room for additional *primordial* small x gluons, distinct from the usual WW dressing of valence quarks we used.

Note added in proof

In Sec. IV E we have iterated instanton-induced multigluon rescattering and derived the expression (55), predicting a peak near the sphaleron mass and restoring one power of instanton diluteness. It has been brought to our attention that a rather different approach based on instanton field modification has been used by Diakonov and Petrov [30]. The results, summarized in the last figure of their paper, are in very good agreement with our result (55).

It has been pointed out by Shuryak [31] that the mechanism of prompt multiparton production considered in this paper may be very important for high energy (heavy ion) collisions, especially in the Realitivistic Heavy Ion Collider energy range. Prompt entropy production is crucial for understanding quark-gluon plasma formation and its collective behavior at early stages of the process.

ACKNOWLEDGMENTS

This work was supported in part by the U.S. DOE grant DE-FG-88ER40388 and by the Polish Government Project (KBN) 2P03B 00814.

[1] A. A. Belavin, A. M. Polyakov, A. A. Schwartz, and Y. S. Tyupkin, Phys. Lett. **59B**, 85 (1975); G. 't Hooft, Phys. Rev. D **14**, 3432 (1976).
[2] C. G. Callan, R. Dashen, and D. J. Gross, Phys. Rev. D **17**, 2717 (1978).
[3] T. Schafer and E. V. Shuryak, Rev. Mod. Phys. **70**, 323 (1998), and references therein.
[4] E. Kuraev, L. Lipatov, and V. Fadin, Sov. Phys. JETP **45**, 199 (1977); I. Balitsky and L. Lipatov, Sov. J. Nucl. Phys. **28**, 822 (1978); L. Lipatov, Sov. Phys. JETP **63**, 904 (1986).
[5] O. Nachtmann, Ann. Phys. (N.Y.) **209**, 436 (1991); hep-ph/9609365.
[6] A. Muller, Nucl. Phys. **B335**, 115 (1990).
[7] E. V. Shuryak, Phys. Lett. B **486**, 378 (2000).
[8] D. Kharzeev and E. Levin, Nucl. Phys. **B578**, 351 (2000).
[9] D. Kharzeev, Y. Kovchegov, and E. Levin, hep-ph/0007182.
[10] E. Shuryak and I. Zahed, Phys. Rev. D **62**, 085014 (2000).
[11] M. Rho, S. J. Sin, and I. Zahed, Phys. Lett. B **466**, 199 (1999); R. A. Janik and R. Peschanski, Nucl. Phys. **B565**, 193 (2000).
[12] A. Ringwald, Nucl. Phys. **B330**, 1 (1990); O. Espinosa, *ibid.* **B343**, 310 (1990); V. Khoze and A. Ringwald, Phys. Lett. B **259**, 106 (1991); for review, see M. Mattis, Phys. Rep. **214**, 159 (1992).
[13] A. Ringwald and F. Schrempp, Phys. Lett. B **438**, 217 (1998); **459**, 249 (1999).
[14] I. Balitski and A. Yung, Phys. Lett. **168B**, 113 (1986); J. Verbaarschot, Nucl. Phys. **B362**, 33 (1991).
[15] E. V. Shuryak, Nucl. Phys. **B203**, 93 (1982); **B203**, 116 (1982); **B203**, 140 (1982).
[16] V. I. Zakharov, Nucl. Phys. **B353**, 683 (1991).
[17] M. Maggiore and M. Shifman, Phys. Rev. D **46**, 3550 (1992).
[18] F. Low, Phys. Rev. D **12**, 163 (1975).
[19] S. Nussinov, Phys. Rev. Lett. **34**, 1286 (1975).
[20] C. Augier *et al.*, Phys. Lett. B **316**, 448 (1993); N. A. Amos *et al.*, Phys. Rev. Lett. **68**, 2433 (1992).
[21] M. Rueter and H. G. Dosch, Phys. Lett. B **380**, 177 (1996).
[22] A. Donnachie and P. V. Landshoff, Nucl. Phys. **B244**, 322 (1984); **B267**, 690 (1986); Z. Phys. C **61**, 139 (1994).
[23] H. Yamagishi and I. Zahed, ''BRST quantization, strong CP violation, the U(1) problem and θ vacua,'' hep-ph/9507296.
[24] D. Diakonov and V. Y. Petrov, Nucl. Phys. **B245**, 259 (1984).
[25] E. V. Shuryak, ''Probing the boundary of nonperturbative QCD by small size instantons,'' hep-ph/9909458.
[26] T. Schafer and E. V. Shuryak, Phys. Rev. Lett. **75**, 1707 (1995).
[27] L. Randall, R. Rattazzi, and E. Shuryak, Phys. Rev. D **59**, 035005 (1999).

[28] H. G. Dosch, Acta Phys. Pol. B **30**, 3813 (1999); A. Donnachie, H. G. Dosch, and M. Rueter, Phys. Rev. D **59**, 074011 (1999); H. G. Dosch *et al.*, Phys. Lett. B **289**, 153 (1992).
[29] A. E. Dorokhov, S. V. Esaibegian, A. E. Maximov, and S. V. Mikhailov, Eur. Phys. J. C **13**, 331 (2000).
[30] D. Diakonov and V. Petrov, Phys. Rev. D **50**, 266 (1994).
[31] E. Shuryak, ''The instanton/sphaleron mechanism of gluon production and high energy heavy ion collisions at RHIC,'' hep-ph/0101269.